Modifying the endohedral La-ion location in both neutral and positively charged polyhydroxylated metallofullerenes

J. G. Rodríguez-Zavala
Departamento de Ciencias Exactas y Tecnológicas, Centro Universitario de Los Lagos, Universidad de Guadalajara, Enrique Díaz de León S/N, 47460 Jalisco, Mexico

I. Padilla-Osuna* and R. A. Guirado-López†
Instituto de Física "Manuel Sandoval Vallarta," Universidad Autónoma de San Luis Potosí, Alvaro Obregón 64, 78000 San Luis Potosí, Mexico

(Received 19 October 2007; published 24 October 2008)

We present extensive *ab initio* density-functional theory calculations in order to analyze the structure and energetics of both neutral and positively charged highly hydroxylated La@$C_{60}(OH)_{32}^{+q}$ and La@$C_{82}(OH)_{20}^{+q}$ (q=0, 1, 2, 4, 6, and 8) metallofullerenes. Interestingly we obtain, for the neutral hydroxylated structures, that the location of the encapsulated La atom strongly depends on the precise distribution of the OH groups on the carbon surface. Actually, we found atomic configurations in which the La ion is attached to different regions of the inner surface as well as atomic arrays in which weakly bonded endohedral species are obtained, being located near the center of the structure. The previous strong variations in the endohedral position of the lanthanum atom leads to sizable modifications in its valence state as well as to notable changes in the electronic spectra and in the lowest-energy spin configuration of the molecules, which are all facts that could be used to better identify the atomic structure of these highly relevant metallofullerenes. The positive charging (by means of simply electron detachment) of our here-considered La@$C_{60}(OH)_{32}$ compounds reveals that the rupture of various C-C bonds of the carbon network can be achieved. However, even if the previous bond breakage leads to the formation of sizable holes in the C_{60} cavity (made of nine-membered rings), we obtain that the encapsulated La atom was unable to escape from the cage. In contrast, in the polyhydroxylated La@$C_{82}(OH)_{20}$ fullerene, no C-C bond breakage is induced with increasing charge state of the cage, defining thus a more stable molecular compound. The previous results are expected to be of fundamental importance in medical and biological applications where the permanent encapsulation of these highly toxic atomic species is required.

DOI: 10.1103/PhysRevB.78.155426 PACS number(s): 61.48.−c, 72.80.Rj

I. INTRODUCTION

Since their discovery, spheroidal carbon fullerenes have shown to posses a lot of interesting physical and chemical properties that could lead to many important applications, the most notable being in the fields of medicine[1] and biology[2] [as highly efficient magnetic-resonance imaging (MRI) contrast agents and selective drug delivery molecular carriers] as well as in the design of new electronic[3] (novel nanocircuits) and optical[4,5] (photosensitizers and solar cells) devices. Furthermore, it has been clearly established that these cage-shaped structures are also able to accommodate many kinds of atoms[6] and small clusters,[7] giving rise to another exciting field of research named endohedral fullerene chemistry. The previous so-called endofullerene materials have attracted special interest since they are characterized by having unique electronic properties and chemical reactivity, which are not seen in the empty fullerenes.

Actually, at the time of their synthesis, endohedral fullerenes were found to be in general highly unstable in practical applications due to their insolubility and extremely air sensitivity. However, later on, procedures were developed to solubilize (and protect) these kind of carbon compounds by performing the functionalization of its surface with the use of a large variety of small molecules, the most common being the hydroxyl species[8] and carboxilic groups,[9] opening thus new opportunities for potential applications in biomedical and nanomaterials science.

In particular, the use of endohedral polyhydroxylated metallofullerenes $M@C_x(OH)_y$, with M defining metal atoms belonging to the lanthanoid group, has been proposed by several research groups as potential MRI contrast agents.[1] In this case, the entrapment of the previous highly toxic metal atoms within the fullerenes helps to ensure an specially safe *in vivo* use of the molecular compounds since it has been speculated that the carbon cage will protect the encapsulated species from external chemical attack and will prevent also the metal ion release in the body under normal physiological conditions. Actually, the previous carbon complexes have been already administrated to minces[10] and, by reducing the relaxation time of water protons in the effected tissues, they have been found to produce a higher quality diagnostic image when compared to conventional Gd-based contrast agents.

It is important to comment that, although the fundamental properties of a large variety of endohedral metallofullerenes have been extensively investigated in the literature, only a few studies have been reported (at least to the authors knowledge) addressing the stability and electronic behavior of chemically functionalized metallofullerenes.[11] Of course, understanding and controlling the practical applications discussed above require a good knowledge of the precise microstructural features and fundamental physics that occur in these nanometer-sized carbon compounds. As is well known, in our days it is experimentally possible to estimate and iden-

tify the number and type of atomic species present in this kind of water soluble fullerene compounds. However, it is still very difficult to determine the precise geometrical structure of the adsorbed phases adopted by the OH groups on the carbon surface, as well as the exact endohedral location of the encapsulated species, which are of course two factors that are expected to play a fundamental role on the properties observed on a macroscopic scale. In addition, the numerous synthetic routes that are currently used for the fabrication of these types of fullerene derivatives are generally not thermodynamically controlled and thus can allow the preparation of metastable molecular structures that could be also responsible for the appearance of novel phenomena.

Furthermore, with the inclusion of these fullerene derivatives in aqueous environments (or even in the gas phase) it might be also possible to alter the charge state of these carbon compounds, turning them into cationic or anionic molecular species, probably strongly affecting their stability and functionality. In fact, previous theoretical and experimental studies performed on both bare cationic[12] and anionic[13] gas phase $C_{60}^{\pm q}$ fullerenes (with q as large as 12) have already underlined the crucial role played by the amount of excess of positive (or negative) charge $+q$ $(-q)$ on the structure and stability of these kinds of systems. Obviously, the repulsive Coulomb forces become progressively important as q increases and, when they exceed the binding forces, the fullerene could become unstable causing the cage destruction or the partial rupture of the fullerene network.

It is thus clear that (i) the electronic properties of polyhydroxylated metallofullerenes are of computational interest and that (ii) it is of fundamental importance to bring some important details of the atomic structure that go beyond the current experimental evidence. Consequently, systematic theoretical investigations dedicated to analyze the electronic and structural properties of functionalized endohedral metallofullerenes are essential and must be performed in order to shed some more light into the understanding of the measured data.

In this work we systematically study, by means of different density-functional theory (DFT) schemes [i.e., using both extended[14] (pseudopotential approach) and localized[15] (GAUSSIAN03 software) basis sets], the stability and electronic properties of both neutral and positively charged polyhydroxylated $La@C_{60}(OH)_{32}^{+q}$ and $La@C_{82}(OH)_{20}^{+q}$ ($q=0$, 1, 2, 4, 6, and 8) metallofullerenes. We put special emphasis on the influence of different spatial distributions of the OH groups on the two carbon surfaces, as well as on the charge state q of the cages, on the energetics, and on the lowest-energy structure of our considered isomers. On the one hand, we will show how the entrapped metal atom can have different electronic ground states and endohedral locations within the cage depending on the molecular structure of the OH overlayer. On the other hand, our theoretical data will reveal in addition how, by increasing the positive charge in our polyhydroxylated fullerenes (through simply electron detachment), it could be possible to obtain C_{60} cages with sizable holes in the fullerene network as well as to control also the reactivity of the inner carbon surfaces.

The rest of the paper is organized as follows. In Sec. II we briefly describe the theoretical models used for the calculations. In Sec. III we present the discussion of our results. Finally, in Sec. IV the summary and conclusions are given.

II. METHOD OF CALCULATION

We have decided to perform our systematic theoretical investigation by combining two different *ab initio* methodologies.

A. Plane-wave pseudopotential approach

In a first step, the structural properties of our neutral and positively charged polyhydroxylated metallofullerenes will be obtained within the DFT approach using the ultrasoft pseudopotential approximation for the electron-ion interaction and a plane-wave basis set for the wave functions as implemented in the PWSCF code.[14] For all our considered structures, the cutoff energy for the plane-wave expansion is taken to be 476 eV. A cubic supercell with a side dimension of 35 Å was employed in the calculations and the Γ point for the Brillouin-zone integration. In all cases, we use the Perdew-Wang (PW91) gradient corrected functional and we perform fully unconstrained structural optimizations for all our considered isomers using the conjugate gradient method. The convergence in energy was set as 1 meV and the structural optimization was performed until a value of less than 1 meV/Å was achieved for the remaining forces for each atom.

B. Localized basis set methodology

In a second step, we will use the previously obtained low-energy molecular geometries to perform additional single-point DFT calculations with the help of the GAUSSIAN03 software[15] in order to obtain the electronic structure, the charge transfer, and the relative stability between all our considered isomers. In this case, the Kohn-Sham equations will be solved by also considering the Perdew-Wang expression for the exchange-correlation potential together with the Stevens-Basch-Krauss effective core potential (ECP) triple-split basis set,[16] CEP-121G, which is a good compromise between computational costs and accuracy.

We believe that the previous two-step PWSCF/GAUSSIAN03 hybrid procedure will help us to avoid possible inaccuracies related to the periodic repetition of images in the supercell approach. This is expected to be particularly the case when calculating very delicate quantities such as the electronic structure and the total energy (E_{tot}) in our highly charged fullerene compounds. Actually, even if in the PWSCF methodology the study of charged systems is efficiently handled by applying a jellium background charge to maintain the charge neutrality, the use of the GAUSSIAN03 software is expected to give more realistic values for E_{tot}.

The numerical accuracy of the previous hybrid PWSCF/GAUSSIAN03 methodology is tested by calculating some well-known structural and electronic properties of (i) the C_{60} fullerene, (ii) the endohedral $La@C_{60}$ compound, and (iii) the well-known highly stable fullerene diol $C_{60}(OH)_2$,[17] all shown in Fig. 1. The previous results will be then compared with the ones obtained within full PWSCF and GAUSSIAN03

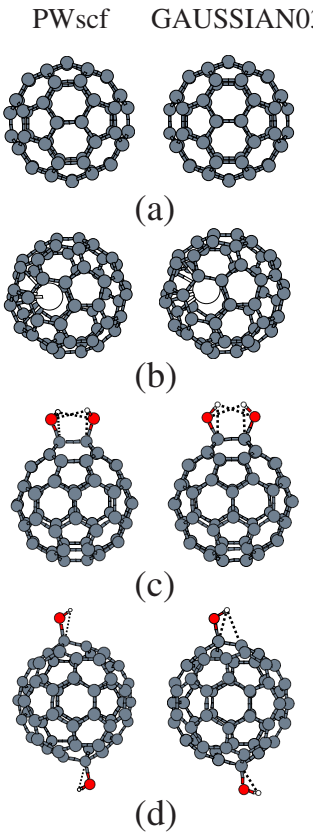

FIG. 1. (Color online) Calculated lowest energy atomic configurations for (a) C_{60} fullerene, (b) La@C_{60} compound, and for [(c) and (d)] two isomers of the $C_{60}(OH)_2$ fullerene diol. In the left (right) column we show results obtained within the PWSCF (GAUSSIAN03) methodology.

treatments. In Fig. 1(a) we show first the optimized structure of the C_{60} molecule obtained within the PWSCF (left) and GAUSSIAN03 (right) methodologies. These lowest-energy atomic configurations have two different C-C bond lengths, being equal to 1.45 (single bond) and 1.40 Å (double bond), calculated within the PWSCF framework, and of 1.47 (single bond) and 1.41 Å (double bond), obtained with the GAUSSIAN03 methodology. These sets of values are in good agreement with gas-phase electron studies (1.458 ± 0.006 and 1.401 ± 0.010 Å) (Ref. 18) and other existing *ab initio* calculations (1.446 and 1.406 Å).[19] In addition, we found highest occupied molecular orbital–lowest unoccupied molecular orbital (HOMO-LUMO) energy gaps Δ_{HL} of 1.74 and 1.65 eV obtained with the GAUSSIAN03 and PWSCF approaches, respectively, both values being very close to the one found with our here-proposed two-step hybrid PWSCF/GAUSSIAN03 methodology that yields a value of 1.8 eV.

For the endohedral La@C_{60} compound shown in Fig. 1(b) we see that, in the equilibrium configuration, the two DFT methodologies reveal that the encapsulated La atom is positioned off center and bonded to the internal surface to approximately six carbon atoms with La-C bonding distances that vary in the range of 2.45–2.88 Å. These values are in good agreement with previous studies addressing the La encapsulation in spheroidal fullerenes.[20] Furthermore, by analyzing the electronic occupations on each site we found, within our two-step PWSCF/GAUSSIAN03 approach, an La $\rightarrow C_{60}$ charge transfer that leaves the encapsulated La species in a positive charge state of +2.11, being also very close to the charge transfer reported for these kinds of systems.[21]

For the fullerene diols shown in Figs. 1(c) and 1(d) we obtain, with both GAUSSIAN03 and PWSCF approaches, that the lowest-energy atomic array corresponds to the structure shown in Fig. 1(c) where the two OH groups are chemisorbed in an on-top configuration above two nearest-neighbors C atoms with a C-O bond length of 1.48 and 1.44 Å, respectively. This configuration is found to be 0.8 (0.74) eV more stable than the one shown in Fig. 1(d) within the GAUSSIAN03 (PWSCF) methodology, an adsorbed phase that is in agreement with the experimentally determined atomic structure for the $C_{60}(OH)_2$ fullerene diol reported by Meier and Kiegiel.[17] The hybrid PWSCF/GAUSSIAN03 calculation predicts the same energy ordering and yields a very similar value for the relative stability of 0.9 eV. Finally we obtain, by using the two DFT types of calculations, a C $\rightarrow$O charge transfer that leaves the oxygen atom negatively charged by −0.69 (GAUSSIAN03) and −0.51 (PWSCF), which are values of the order that the one found with our two-step methodology which is equal to −0.7.

Based on the previous results, we can thus conclude by saying that our hybrid theoretical methodology is appropriate and that it will reasonably describe the stability and electronic properties of our here-considered endohedrally La-doped highly hydroxylated C_{60} and C_{82} fullerenes.

III. RESULTS AND DISCUSSION

A. Polyhydroxylated La@$C_{60}(OH)_{32}^{+q}$ metallofullerenes

We start our study by determining the lowest-energy atomic configurations for some possible highly hydroxylated $C_{60}(OH)_{32}$ isomers. The choice of these types of multihydroxylated fullerene compounds is motivated by the recent experimental work of Xing *et al.*[22] which have synthesized highly stable and highly soluble OH-covered C_{60} molecules with a number of hydroxyl groups that vary in the range of 30–42 OH molecules.

Of course, for the previous degree of surface coverage, it is prohibitively time consuming to categorize the many possibilities in which 32 OH groups can be adsorbed on the C_{60} surface. However, following our previous work[23] in which we have addressed the stability and structural properties of empty highly hydroxylated $C_{60}(OH)_{32}$ fullerenes we have decided to reoptimize—but now at the pseudopotential density-functional level of theory—the three chosen contrasting adsorbed configurations, namely, (i) assuming the existence of small hydroxyl islands on the carbon surface (which has been previously found by us as a highly stable atomic array), (ii) considering a complete aggregation of the OH species on one side of the C_{60} cage, and (iii) assuming the adsorption of 32 OH groups homogeneously distributed on the fullerene surface. The resulting lowest-energy PWSCF structures for the previously proposed initial atomic configurations are shown in Fig. 2. Interestingly and as already obtained in Ref. 23, we found that the formation of small molecular islands on the C_{60} surface [see Fig. 2(a)] corresponds to the most stable

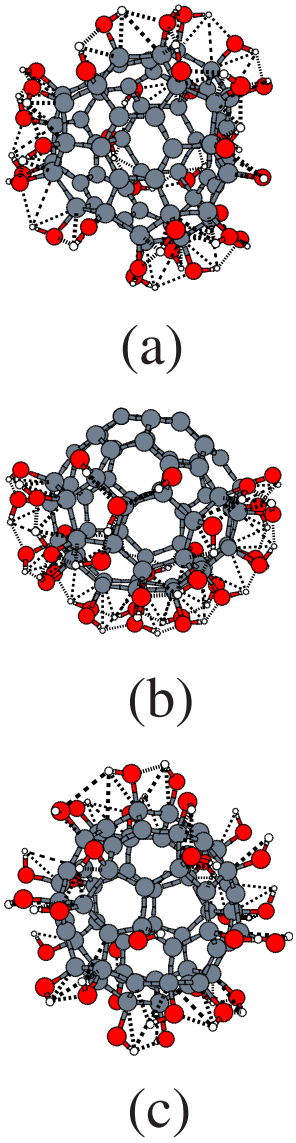

FIG. 2. (Color online) Illustration of the PWSCF lowest energy atomic configurations for three representative $C_{60}(OH)_{32}$ isomers (see text).

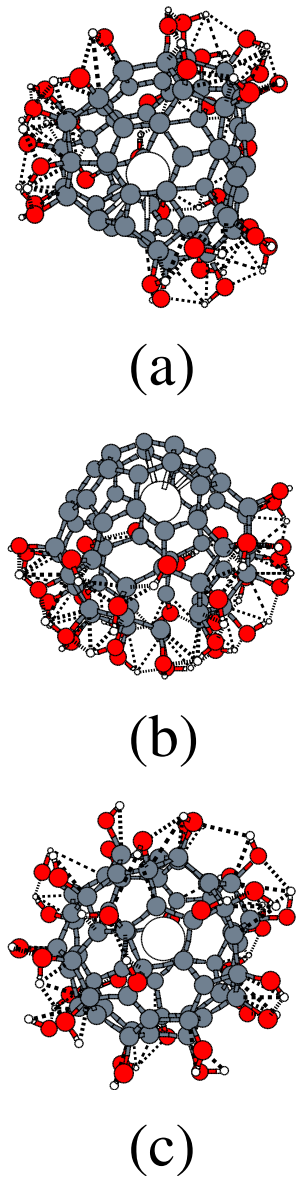

FIG. 3. (Color online) Illustration of the PWSCF lowest energy atomic configurations for our considered $La@C_{60}(OH)_{32}$ compounds (see text).

adsorbed phase. In this case (and as found before within the PM3 Hamiltonian) we obtain the formation of a highly orientationally ordered OH molecular overlayer, being characterized by the existence of localized networks of hydrogen bonds between neighboring OH groups (see the dotted lines). Notice that this orientational order (in which the positively charged H atoms are always pointing toward their nearest negatively charged O species) is maintained in the segregated phase [see Fig. 2(b)]; however, it is in contrast considerably lost in the (less stable) homogeneous distribution of OH groups, being thus an important factor for determining the structural stability in these kind of systems.

From Fig. 2 we notice that, in all cases, the OH groups are always adsorbed in an on-top configuration above the carbon atoms of the C_{60} with C-O and O-H bond lengths of 1.40–1.46 and 0.97–1.01 Å, respectively, as well as C-O-H angles that vary in the range of 99°–106°. In addition, we observe that the hydroxylation of the fullerene surface considerably perturbs the structure of the underlying carbon network since the C atoms just below the OH groups perform upward as well as lateral displacements in order to minimize the total energy of the system. However, despite the existence of these complex atomic relaxations, we note that no C-C bond breakage in the carbon network is obtained. Actually, if we compare with our previous results addressing the structural properties of low[24] and medium[25] OH-covered C_{60} fullerenes, our results presented in this work clearly support the experimental observation of Xing *et al.*[22] which have found that the structural stability of highly hydroxylated C_{60} is not so sensitive to the number of adsorbed OH groups.

In Fig. 3 we show the lowest-energy PWSCF atomic configurations for the fullerene isomers shown in Fig. 2 but now containing an encapsulated La atom. First it is important to comment that the inclusion of the lanthanum atom does not

modify the relative stability between all our considered isomers, being again the most stable La@$C_{60}(OH)_{32}$ molecular compound the one in which a patchy behavior for the OH groups on the carbon surface is obtained [see Fig. 3(a)]. From the figures we also see that the hydrogen bonded network stabilizing the molecular overlayers shown in Figs. 2(a) and 2(b) is still stable after the endohedral doping (even in regions around the La-adsorption site) [see Fig. 3(a)]. In fact, the OH molecular coating is characterized by R_{C-O} and R_{O-H} bond lengths which vary in the range of 1.41–1.46 and 0.98–1.01 Å, respectively, together with C-O-H angles of 103°–106°, all of them being of the order of the values found in the empty cages (see Fig. 2).

However, the most important feature to remark from Fig. 3 is that the encapsulated La atom clearly changes its endohedral location when the structure of the molecular overlayer is modified. From Figs. 3(a) and 3(b) we can see that the lanthanum atom prefers to be adsorbed in the uncovered regions of the C_{60} surface, with La-C bond lengths that vary in the range of 2.43–2.84 Å, as in the unprotected fullerene cage shown in Fig. 1(b). In fact, this trend is corroborated in Fig. 3(c) where, for an homogeneous distribution of hydroxyl groups on the C_{60} surface, extended uncovered carbon regions are difficult to find. In that case, notice that the encapsulated La atom prefers thus to be placed now far away from the internal surface (being located near the center of the structure), the closets La-C interatomic distance being equal to 2.71 Å. It is thus evident that for different coverages and geometrical details of the adsorbed molecular overlayer we will have contrasting guest-host interactions (and a different dynamic behavior for the confined La atom) that surely will be of fundamental importance to understand the electronic behavior of these molecular compounds. Finally, we believe that the previous sizable variations in the La-C interatomic distances found in Fig. 3 could be reflected in infrared spectroscopy measurements of these kinds of samples. Of course, a broad distribution of R_{La-C} values is expected to lead to different (in position and intensity) La-C vibrational contributions, and could be thus very helpful to better identify the structural features of these molecular compounds.

As in the case of Fig. 1(b) we always found in all the structures shown in Fig. 3 a sizable La→C charge transfer. However, we have obtained, within the PWSCF/GAUSSIAN03 methodology, that the amount of transferred charge varies as a function of the adsorbed configuration on the inner surface. Actually, by performing a natural population analysis (which is better than the Mulliken method in the case of metallofullerenes[26]) we have found that the charge state of the La atom is equal to +1.96, +2.22, and +2.01 in Figs. 3(a)–3(c), respectively. Of course, stripped of ~2 electrons the metal ion is naturally always attracted by the electron-rich portions of the fullerene surface which, as shown in Fig. 3, are defined by the uncovered carbon regions of the molecular compounds.

Furthermore the previous charge transfer induces, as expected, strong variations in the electronic spectra of the molecules, mainly in the energy region around the highest occupied molecular orbital. This is actually what we see from Fig. 4 where we plot, as a representative example, the spin-polarized energy-level distribution (obtained within the PWSCF/GAUSSIAN03 framework) for the lowest energy La@$C_{60}(OH)_{32}$ compound shown in Fig. 3(a) and in which we only include the 11 occupied molecular orbitals with the highest energies, and of the 11 unoccupied molecular orbitals with the lowest energies. For the sake of comparison we also show the electronic structure of the corresponding empty $C_{60}(OH)_{32}$ cage [Fig. 2(a)]. From the figure we have found (if we compare with the La-free molecular compounds) that sizable modifications in the eigenvalue spectra around the HOMO are obtained, consisting in various displacements and splittings (changes in the degeneracy) of the energy levels. It is important to comment that, besides the important role played by the large amount of La→C transferred charge, there are also non-negligible contributions to the precise details of the energy-level distribution shown in Fig. 4 from the structural distortions in the carbon network induced upon La-adsorption. Even if the previous geometrical perturbations are localized in nature, they lower the symmetry of the molecular structure and reduce still further the degeneracy of the electronic spectra.

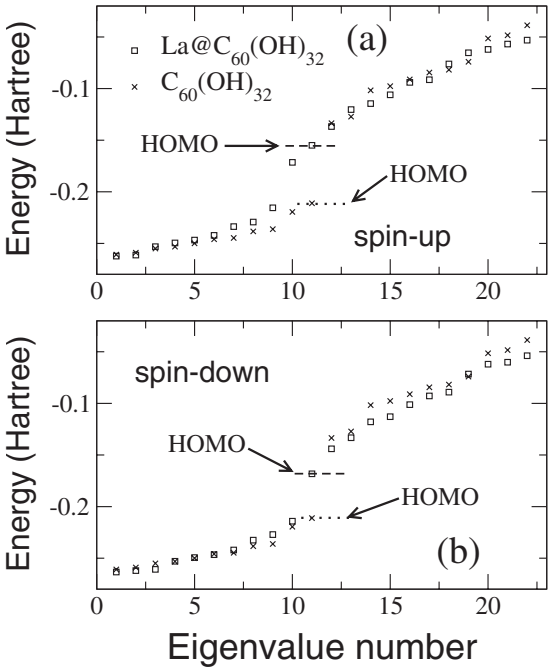

FIG. 4. Comparison of the eigenvalue spectra (obtained with the hybrid PWSCF/GAUSSIAN03 approach) for the empty and La-doped $C_{60}(OH)_{32}$ fullerenes shown in Figs. 2(a) and 3(a), respectively. In the figure, we show results for both (a) spin-up and (b) spin-down distributions. We only include the 11 occupied molecular orbitals with the highest energies and the 11 unoccupied molecular orbitals with the lowest energies. The energy location of the HOMO for the empty (endohedrally-doped) molecular compound is marked with a horizontal doted (dashed) line.

It is important to precise that the energy gap Δ_{HL} of 0.3 eV calculated from Fig. 4 is obtained between the HOMO of spin-up character [Fig. 4(a)] and the LUMO of spin-down nature [Fig. 4(b)]. The different spin nature of the HOMO and LUMO levels is of course a consequence of the odd number of electrons present in the system due to the inclusion of the La atom, a fact that defines also the existence of

a weakly magnetic molecular structure. Actually, the isomers shown in Figs. 3(a) and 3(b) have a total spin magnetization of $1\mu_B$ while, in the molecular compound shown in Fig. 3(c), in which the La ion is more weakly bonded to the internal carbon surface, the total energy decreases with increasing the spin multiplicity, leading to a total spin moment of $3\mu_B$. Finally, it is important to comment that our lowest energy La-containing hydroxylated fullerene shown in Fig. 3(a) is expected to be still stable with increasing temperature since, as has been demonstrated by Tozzini *et al.*,[27] the thermal stability of fullerenelike structures is strongly correlated with the width of their electronic energy gap.

As is well known, from the spectroscopic point of view, variations in Δ_{HL} between the different isomers shown in Figs. 2 and 3 should be reflected in the optical properties of the samples. In fact, it has been demonstrated that molecular structures with reduced (large) electronic energy gaps are expected to have their first optical excitations around the infrared (ultraviolet) region of the absorption spectra, providing a finger print to identify the structure of these kind of synthesized fullerene compounds.[25] To verify the previous assumption, we will perform additional time-dependent DFT calculations (with the use of the GAUSSIAN03 methodology at the Perdew-Wang-91/CEP-121G level of theory) on the two most stable atomic configurations shown in Figs. 2 and 3, in order to determine their optical gap (defined as the first single dipole-allowed excitation) which strongly depends on the precise details of the energy-level distribution around the HOMO. As stated by Xie *et al.*,[5] calculations of the first single dipole-allowed excitation of the C_{60} molecule using this exchange-correlation functional yield values which are in very good agreement with the ones experimentally obtained from dilute C_{60} solutions (e.g., hexane, benzene, toluene, etc.) and with those reported by other DFT calculations.

In the case of the hydroxylated structures shown in Figs. 2(a) and 2(b) we found, in agreement with our previous work, that the formation of small OH molecular domains on the fullerene surface induces a notable redshift in the optical gap, with respect to the one obtained in the uncovered C_{60}, being now placed at 2.31 eV (~535 nm). However, in the segregated configuration [Fig. 2(b)] we observe a more pronounced displacement, the first single dipole-allowed excitation being now located at 1.43 eV (~865 nm). It is clear that our time-dependent DFT calculations reveal big differences between the two considered isomers and that the previous features clearly provide a fingerprint that could be very useful to identify the possible structure of these types of fullerene derivatives.

The situation is much more interesting in the La-containing $C_{60}(OH)_{32}$ compounds shown in Figs. 3(a) and 3(b). In both cases, we note that the inclusion of the lanthanum atom induces a dramatic redshift in the location of the optical gap, being now placed in the far-infrared region, i.e.; 0.53 eV (~2342 nm) in Fig. 3(a) and 0.37 eV (~3360 nm) for Fig. 3(b). It is thus clear that since $C_{60}(OH)_{32}$ and $La@C_{60}(OH)_{32}$ strongly differ in their optical gaps, ranging from the near-infrared to the far-infrared region, they may be used not only as novel nanocontainers but also like single molecule optical probes as labeling, detection, and identification agents.

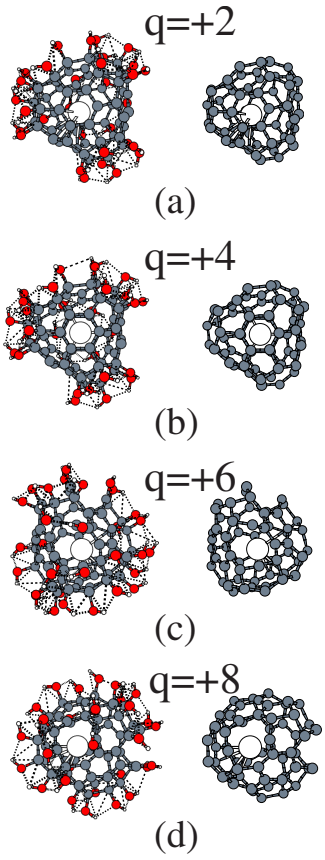

FIG. 5. (Color online) Illustration of the PWSCF lowest energy atomic configurations for the $La@C_{60}(OH)_{32}^{+q}$ molecular compound shown in Fig. 3(a) having different charge states q. To the right of each one of the equilibrium configurations obtained we show in addition the structure of the underlying carbon network (by removing all the OH groups from the surface) in order to appreciate the structural deformations induced on the fullerene cavity.

At this point, and as stated in Sec. I of the paper, we must comment that the inclusion of the fullerene structures shown in Fig. 3 in real environments could lead to a sizable positive charging of the molecular compounds through simple electron detachment (in the gas phase) or by the adsorption of atomic impurities (in solution studies). Consequently, and from the point of view of applications, it is thus of fundamental importance to analyze also the structural stability of both the carbon network and of the adsorbed OH molecular coating for different charge states. The previous studies are particularly important in view of the large variety of possible medical uses in which the inclusion of various endohedrally-doped polyhydroxylated fullerenes into the human body is required. As is well known, atoms belonging to the lanthanoid group as well as carbon fullerenes with bare surfaces can be highly toxic (causing significant cell death)[28] and, as a consequence, it is thus necessary to prevent the metal ion release or the desorption (degradation) of the protective hydroxyl layer within the human body.

In Fig. 5 we present thus the lowest energy PWSCF atomic configuration of the most stable fullerene compound shown in Fig. 3(a) but having different charge states $+q$. In the figure, we show our fully optimized $La@C_{60}(OH)_{32}^{+q}$ com-

pounds, where q will be as large as 8, which is a reasonable charge state that can be easily experimentally achieved.[12] We show also in addition, to the right of each one of the equilibrium configurations, only the structure of the corresponding underlying carbon network in order to more clearly appreciate the structural deformations induced on the C_{60} cavity by the charging of the systems. From the figures the most important features to remark are that, similar to the results shown in Fig. 3, (i) the La-ion changes its endohedral location but now when the q value increases and that, as already found in Ref. 23, (ii) the charging of the fullerene compound (up to $q=+8$) induces the rupture of various C-C bonds of the carbon network, leading to the formation of sizable holes in the C_{60} cavity made of nine-membered rings [see Figs. 5(c) and 5(d)]. However, it is interesting to remark that these holes are not attractive for the encapsulated species. In fact, notice from the figures that the confined La-ion is found to be always adsorbed away from these openings, being still stable in the inside of our partially open carbon cages. Actually, we have performed additional calculations in which we have readsorbed the lanthanum atom precisely above all the nine-membered rings shown in Figs. 5(c) and 5(d) and, during the optimization process, the La ion always desorbs from this area and moves to a nearest and uncovered carbon region, ending up finally attached in an on-hollow configuration over a six-membered ring.

It is reasonable to expect that with increasing the charge state in the molecular compounds more complex structural rearrangements will occur, possibly leading to the presence of bigger holes in the fullerene cavity. In addition, with the encapsulation of smaller atomic species, ion-scape through the defect could more probably occur. At this point, we would like to remark that the role of the presence of holes in a fullerene cage on the metal ion migrations remains mostly unexplored. Of course additional studies analyzing possible reaction pathways, as well as the estimation of the magnitude of the energy barriers that need to be overcome, are necessary in order to more clearly understand the conditions by which the encapsulated species could be ejected through the defect. Some of these calculations are currently in progress.

Finally, we can thus conclude this section by saying that the most possible structure of cationic $La@C_{60}(OH)_{32}^{+q}$ species is in the form of open cage configurations. It is also clear that, in these kinds of highly hydroxylated fullerene compounds, the control of the amount of missing electrons could be very useful for modifying the endohedral location of the encapsulated species as well as the size of the opening of the cage.

B. Polyhydroxylated $La@C_{82}(OH)_{20}^{+q}$ metallofullerenes

We present now the lowest energy PWscf atomic configurations for some possible highly hydroxylated $C_{82}(OH)_{20}$ isomers. In this case, the amount of OH groups covering the carbon structure has been chosen following the recent experimental work of Chen *et al.*[29] in which the synthesis of polyhydroxylated $C_{82}(OH)_{22}$ structures has been reported.

As in the previous section, we consider again (i) OH groups distributed on the surface forming small molecular islands, (ii) hydroxyl molecules completely aggregated on one side of the C_{82} cage, and (iii) assuming the adsorption of 20 OH groups homogeneously distributed on the fullerene surface. The resulting PWSCF lowest energy structures for the previously proposed initial atomic configurations are shown in Fig. 6. Interestingly, as already obtained in Ref. 23 and in this work, we found that the formation of small molecular islands on the C_{82} surface [see Fig. 6(a)] corresponds to the most stable adsorbed phase. We notice also the formation of localized networks of hydrogen bonds between neighboring OH groups (see the dotted lines) in good agreement with our previous calculations.

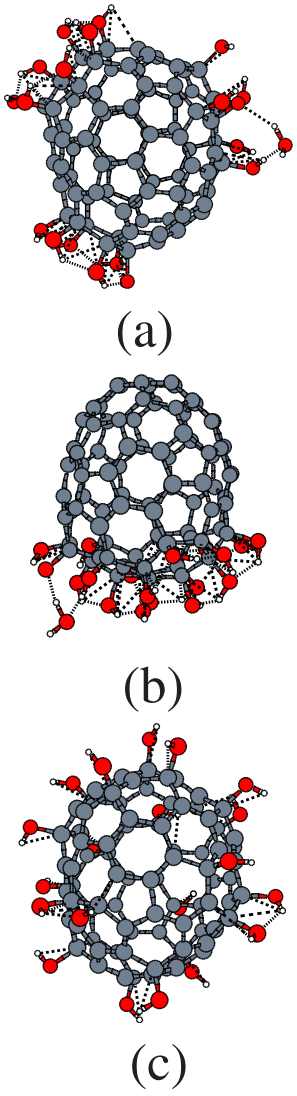

FIG. 6. (Color online) Illustration of the PWSCF lowest energy atomic configurations for three representative $C_{82}(OH)_{20}$ isomers (see text).

It is important to remark that even if the configuration shown in Fig. 6(a) is the most stable array, the segregated structure in Fig. 6(b) is (in contrast to the results of Fig. 2) only located 0.1 eV above in energy, being thus the two of them almost degenerate. This result is very interesting and clearly precludes a complex interplay between the relative stability, the size and symmetry of the carbon cage, as well

as the degree of surface OH coverage in these kinds of molecular compounds. Finally, and also in contrast to Fig. 2, we notice from Figs. 6(a) and 6(b) the existence of more complex lateral interactions between the coadsorbed hydroxyl groups. In both OH-covered C_{82} isomers, we can clearly see that the close proximity between two OH species can induce a favorable attraction that originates the formation of water molecules. From the figures we note that the H_2O species desorb from the molecular coating; however, they are found to be still physisorbed on the hydroxylated (hydrophilic) parts of the carbon structure. Interestingly, this process also induces the contamination of the fullerene surface due to the existence of chemisorbed atomic oxygen resulting from the $OH+OH \rightarrow H_2O+O$ reaction.

In Fig. 7 we present now the lowest energy PWSCF atomic configurations for the $C_{82}(OH)_{20}$ fullerene isomers shown in Fig. 6 but now containing an encapsulated La atom. As a reference, in Fig. 7(a) we show first the lowest energy structure for the uncovered $La@C_{82}$ endohedral metallofullerene. From the figure we notice again that the center is an unstable position for the La atom. As in the C_{60} cage [see Fig. 1(b)] the lanthanum atom is found to be attached to the internal carbon surface, being close to a double C-C bond, with an La-C interatomic distance distribution that varies in the range of 2.43–2.65 Å (being of the order of the ones reported previously by Poirier *et al.*[20]). Interestingly, and in contrast to Fig. 3, in the polyhydroxylated C_{82} cages the inclusion of the lanthanum atom modifies the relative stability between our three considered isomers. Now, the atomic array in which a segregated configuration for the OH groups on the carbon surface is assumed [see Fig. 7(c)] is found to be 1.2 eV more stable (within our hybrid PWSCF/GAUSSIAN03 approach) that the one in which OH-island formation is observed [Fig. 7(b)]. Furthermore, by comparing the lowest energy atomic arrays shown in Figs. 7(b)–7(d) we can clearly see that the endohedral location of the La atom strongly depends also on the structure of the adsorbed molecular OH coating. From the figures we see notable displacements of the encapsulated La species on the inner carbon surface which are clearly reflected in its charge state, changing from +2.1 [Fig. 7(b)] to +2.3 [Fig. 7(c)] to +2.2 [Fig. 7(d)].

Finally, it is important to briefly comment also on the effect of increasing the positive charge in our $La@C_{82}(OH)_{20}^{+q}$ molecular compounds. Interestingly and in contrast to the results shown in Fig. 5 we have found (not shown) that, even if considering values of q as large as 8, (i) no C-C bond breakage in the carbon network is obtained, (ii) only minor structural deformations to the C_{82} cage are induced, and (iii) small displacements of the encapsulated La atom adsorbed on the inner surface are found. These results are of fundamental importance and define thus the hydroxylated C_{82} fullerene as a more appropriate structure for protecting the encapsulated species from external chemical attack or metal ion release in the body.

IV. SUMMARY AND CONCLUSIONS

In this work, we have presented a systematic *ab initio* density-functional theory investigation dedicated to analyze the stability as well as electronic properties of both neutral and positively charged polyhydroxylated $La@C_{60}(OH)_{32}^{+q}$ and $La@C_{82}(OH)_{20}^{+q}$ ($q=0,2,4,6,8$) metallofullerenes. We have obtained that the endohedral location of the lanthanum atom strongly depends on the precise distribution of the OH groups on the carbon surfaces. In particular, we have found that there is a favorable attraction between the encapsulated La ion and the electron-rich (uncovered) regions of the carbon network, a fact that leads to the existence of well defined adsorbed configurations within the cavities. Interestingly, the previous adsorbed phases are characterized by different La-C

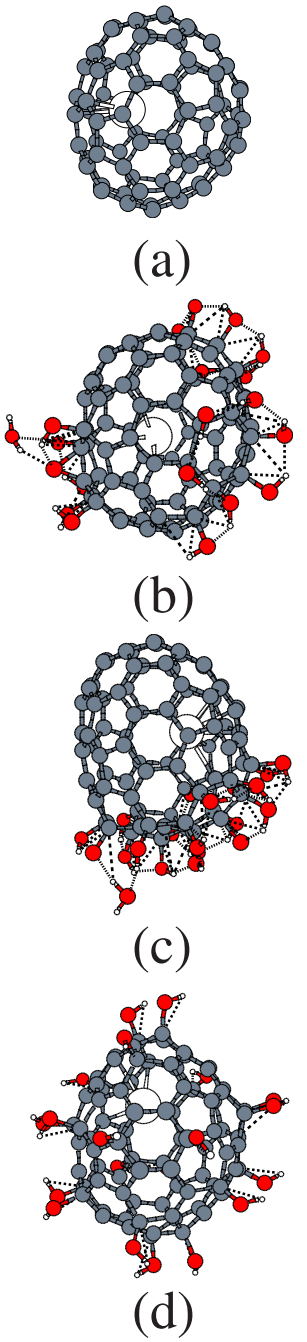

FIG. 7. (Color online) Illustration of the PWSCF lowest energy atomic configurations for our considered $La@C_{82}(OH)_{20}$ compounds (see text).

bond lengths and by having a contrasting distribution of the energy levels around the highest occupied molecular orbital. In addition, notable variations in the total spin magnetization and in the charge state of the encapsulated species are also found, which are all facts that could be used to better identify the possible atomic configuration of these molecular compounds.

Finally, we have obtained that by positively charging our polyhydroxylated C_{60} metallofullerenes it is possible to induce the rupture of various C-C of the carbon network, a fact that leads to the formation of sizable holes in the fullerene cavities. However, in all cases, we have found that the encapsulated La ion was still stable in the inside of our partially open carbon cages. In contrast, in the hydroxylated C_{82}-based endohedral fullerenes, no C-C bond breakage in the carbon cage is obtained. The previous results are expected to be of fundamental importance in medical and biological applications where the permanent encapsulation of highly toxic atomic species is required.

ACKNOWLEDGMENTS

The authors would like to acknowledge the financial support from CONACyT through Grants No. 45928-F and No. 50050 (R.A.G.-L.) as well as from PROMEP (J.G.R.-Z. and R.A.G.-L.). Finally, computational resources from the Instituto Potosino de Investigación Científica y Tecnológica (IPICyT), SLP, México, are also acknowledged.

*ismael@ifisica.uaslp.mx
†guirado@ifisica.uaslp.mx

[1] B. Sitharaman, R. D. Bolskar, I. Rusakova, and L. J. Wilson, Nano Lett. **4**, 2373 (2004); H. Kato, Y. Kanazawa, M. Okumura, A. Taninaka, T. Yokawa, and H. Shinohara, J. Am. Chem. Soc. **125**, 4391 (2003); E. Tóth, R. D. Bolskar, A. Borel, G. González, L. Helm, A. E. Merbach, B. Sitharaman, and L. J. Wilson, *ibid.* **127**, 799 (2005).

[2] E. Nakamura and H. Isobe, Acc. Chem. Res. **36**, 807 (2003); S. H. Friedman, D. L. DeCamp, R. P. Sijbesma, G. Srdanov, F. Wudl, and G. L. Kenyon, J. Am. Chem. Soc. **115**, 6506 (1993).

[3] L. Senapati, J. Schrier, and K. B. Whaley, Nano Lett. **4**, 2073 (2004).

[4] J. W. Arbogast, A. P. Darmanyan, C. S. Foote, M. M. Alvarez, S. J. Anz, and R. L. Whetten, J. Phys. Chem. **95**, 11 (1991); J. W. Arbogast and C. S. Foote, J. Am. Chem. Soc. **113**, 8886 (1991).

[5] R.-H. Xie, G. W. Bryant, G. Sun, M. C. Nicklaus, D. Heringer, Th. Frauenheim, M. Riad Manaa, V. H. Smith, Y. Araki, and O. Ito, J. Chem. Phys. **120**, 5133 (2004).

[6] E. Nishibori, K. Iwata, M. Sakata, M. Takata, H. Tanaka, H. Kato, and H. Shinohara, Phys. Rev. B **69**, 113412 (2004); V. K. Dolmatov and S. T. Manson, Phys. Rev. A **73**, 013201 (2006); M. Yamada, L. Feng, T. Wakahara, T. Tsuchiya, Y. Maeda, Y. Lian, M. Kako, T. Akasaka, T. Kato, K. Kobayashi, and S. Nagase, J. Phys. Chem. B **109**, 6049 (2005).

[7] M. Krause, X. Liu, J. Wong, T. Pichler, M. Knupfer, and L. Dunsch, J. Phys. Chem. A **109**, 7088 (2005); C. M. Cardona, A. Kitaygorodskiy, and L. Echegoyen, J. Am. Chem. Soc. **127**, 10448 (2005); B. Cao, K. Suenaga, T. Okazaki, and H. Shinohara, J. Phys. Chem. B **106**, 9295 (2002); N. Chen, E. Y. Zhang, and C. R. Wang, *ibid.* **110**, 13322 (2006).

[8] W.-L. Liu, U. Jeng, T.-L. Lin, S.-H. Lai, M. C. Shih, C.-S. Tsao, L. Y. Wang, L. Y. Chiang, and L. P. Sung, Physica B (Amsterdam) **283**, 49 (2000); C. Chen, G. Xing, J. Wang, Y. Zhao, B. Li, J. Tang, G. Jia, T. Wang, J. Sun, L. Xing, H. Yuan, Y. Gao, H. Meng, Z. Chen, F. Zhao, Z. Chai, and X. Fang, Nano Lett. **5**, 2050 (2005); L. O. Husebo, B. Sitharaman, K. Furukawa, T. Kato, and L. J. Wilson, J. Am. Chem. Soc. **126**, 12055 (2004).

[9] R. D. Bolskar, A. F. Benedetto, L. O. Husebo, R. E. Price, E. F. Jackson, S. Wallace, L. J. Wilson, and J. M. Alford, J. Am. Chem. Soc. **125**, 5471 (2003); S. Laus, B. Sitharaman, É. Tóth, R. D. Bolskar, L. Helm, S. Asokan, M. S. Wong, L. J. Wilson, and A. E. Merbach, *ibid.* **127**, 9368 (2005).

[10] M. Mikawa, H. Kato, M. Okumura, M. Narazaki, Y. Kanazawa, N. Miwa, and H. Shinohara, Bioconjugate Chem. **12**, 510 (2001).

[11] M. Yamada, T. Wakahara, T. Nakahodo, T. Tsuchiya, Y. Maeda, T. Akasaka, K. Yoza, E. Horn, N. Mizorogi, and S. Nagase, J. Am. Chem. Soc. **128**, 1402 (2006); L. Feng, T. Nakahodo, T. Wakahara, T. Tsuchiya, Y. Maeda, T. Akasaka, T. Kato, E. Horn, K. Yoza, N. Mizorogi, and S. Nagase, *ibid.* **127**, 17136 (2005); M. Yamada, T. Nakahodo, T. Wakahara, T. Tsuchiya, Y. Maeda, T. Akasaka, M. Kako, K. Yoza, E. Horn, N. Mizorogi, K. Kobayashi, and S. Nagase, *ibid.* **127**, 14570 (2005).

[12] S. Díaz-Tendero, M. Alcamí, and F. Martín, Phys. Rev. Lett. **95**, 013401 (2005); T. Bastug, P. Kürpick, J. Meyer, W. D. Sepp, B. Fricke, and A. Rosén, Phys. Rev. B **55**, 5015 (1997); T. Majima, Y. Nakai, H. Tsuchida, and A. Itoh, Phys. Rev. A **69**, 031202(R) (2004).

[13] O. T. Ehrler, F. Furche, J. M. Weber, and M. M. Kappes, J. Chem. Phys. **122**, 094321 (2005).

[14] S. Baroni, A. Dal Corso, S. de Gironcoli, P. Giannozzi, C. Cavazzoni, G. Ballabio, S. Scandolo, G. Chiarotti, P. Focher, A. Pasquarello, K. Laasonen, A. Trave, R. Car, N. Marzani, and A. Kokalj (http://www.pwscf.org/).

[15] M. J. Frisch *et al.*, GAUSSIAN 03, Revision C.02, Gaussian, Inc., Wallingford, CT, 2004.

[16] W. Stevens, H. Basch, and J. Krauss, J. Chem. Phys. **81**, 6026 (1984); W. J. Stevens, M. Krauss, H. Basch, and P. G. Jasien, Can. J. Chem. **70**, 612 (1992); T. R. Cundari and W. J. Stevens, J. Chem. Phys. **98**, 5555 (1993).

[17] M. S. Meier and J. Kiegel, Org. Lett. **3**, 1717 (2001).

[18] K. Hedberg, L. Hedberg, D. S. Bethune, C. A. Brown, H. C. Dorn, R. D. Johnson, and M. de Vires, Science **254**, 410 (1991).

[19] M. Haser, J. Almlof, and G. E. Scuseria, Chem. Phys. Lett. **181**, 497 (1991).

[20] D. M. Poirier, M. Knupfer, J. H. Weaver, W. Andreoni, K. Laasonen, M. Parrinello, D. S. Bethune, K. Kikuchi, and Y. Achiba, Phys. Rev. B **49**, 17403 (1994); P. Jin, C. Hao, S. Li, W. Mi, Z. Sun, J. Zhang, and Q. Hou, J. Phys. Chem. A **111**, 167 (2007).

[21] A. H. H. Chang, W. C. Ermler, and R. M. Pitzer, J. Chem. Phys. **94**, 5004 (1991); J. Lu, X. Zhang, and X. Zhao, Appl. Phys. A:

Mater. Sci. Process. **70**, 461 (2000).
[22] G. Xing, J. Zhang, Y. Zhao, J. Tang, B. Zhang, X. Gao, H. Yuan, L. Qu, W. Cao, Z. Chai, K. Ibrahim, and R. Su, J. Phys. Chem. B **108**, 11473 (2004).
[23] J. G. Rodríguez-Zavala and R. A. Guirado-López, J. Phys. Chem. A **110**, 9459 (2006).
[24] J. G. Rodríguez-Zavala and R. A. Guirado-López, Phys. Rev. B **69**, 075411 (2004).
[25] R. A. Guirado-López and M. E. Rincón, J. Chem. Phys. **125**, 154312 (2006).
[26] J. Lu, W. N. Mei, Y. Gao, X. Zeng, M. Jing, G. Li, R. Sabirianov, Z. Gao, L. You, J. Xu, D. Yu, and H. Ye, Chem. Phys. Lett. **425**, 82 (2006).
[27] V. Tozzini, F. Buda, and A. Fasolino, Phys. Rev. Lett. **85**, 4554 (2000).
[28] L. Ding, J. Stilwell, T. Zhang, O. Elboudwcrej, K. Jiang, J. P. Selegue, P. A. Cooke, J. W. Gray, and F. F. Chen, Nano Lett. **5**, 2448 (2005); C. M. Sayes, J. D. Fortner, W. Guo, D. Lyon, A. M. Boyd, K. D. Ausman, Y. J. Tao, B. Sitharaman, L. J. Wilson, J. B. Hughes, J. L. West, and V. L. Colvin, *ibid.* **4**, 1881 (2004).
[29] C. Chen, G. Xing, J. Wang, Y. Zhao, B. Li, J. Tang, G. Jia, T. Wang, J. Sun, L. Xing, H. Yuan, Y. Gao, H. Meng, Z. Chen, F. Zhao, Z. Chai, and X. Fang, Nano Lett. **5**, 2050 (2005).